*HIPPOCAMPUS 6:294–305 (1996)*

# Physiological Properties of Anatomically Identified Basket and Bistratified Cells in the CA1 Area of the Rat Hippocampus In Vitro

Eberhard H. Buhl,[1] Tibor Szilágyi,[1,2] Katalin Halasy,[1,3] and Peter Somogyi[1]

*[1]MRC Anatomical Neuropharmacology Unit, Oxford University, Oxford, England; [2]Department of Physiology, University of Medicine and Pharmacy, Tirgu Mures, Romania; [3]Department of Zoology and Cell Biology, József Attila University, Szeged, Hungary*

**ABSTRACT: Basket and bistratified cells form two anatomically distinct classes of GABAergic local-circuit neurons in the CA1 region of the rat hippocampus. A physiological comparison was made of intracellularly recorded basket (n = 13) and bistratified neurons (n = 6), all of which had been anatomically defined by their efferent target profile (Halasy et al., 1996).**

**Basket cells had an average resting membrane potential of −64.2 ± 7.2 vs. −69.2 ± 4.6 mV in bistratified cells. The latter had considerably higher mean input resistances (60.2 ± 42.1 vs. 31.3 ± 10.9 MΩ) and longer membrane time constants (18.6 ± 8.1 vs. 9.8 ± 4.5 ms) than basket cells. Differences were also apparent in the duration of action potentials, those of basket cells being 364 ± 77 and those of bistratified cells being 527 ± 138 μs at half-amplitude. Action potentials were generally followed by prominent, fast afterhyperpolarizing potentials which in basket cells were 13.5 ± 6.7 mV in amplitude vs. 10.5 ± 5.1 in bistratified cells. The differences in membrane time constant, resting membrane potential, and action potential duration reached statistical significance ($P < 0.05$).**

**Extracellular stimulation of Schaffer collateral/commissural afferents elicited short-latency excitatory postsynaptic potentials (EPSPs) in both cell types. The average 10–90% rise time and duration (at half-amplitude) of subthreshold EPSPs in basket cells were 1.9 ± 0.5 and 10.7 ± 5.6 ms, compared to 3.3 ± 1.3 and 20.1 ± 9.7 ms in bistratified cells, the difference in EPSP rise times being statistically significant. Basket and bistratified EPSPs were highly sensitive to a bath applied antagonist of non-*N*-methyl-D-aspartate (NMDA) receptors, whereas the remaining slow-rise EPSP could be abolished by an NMDA receptor antagonist. Increasing stimulation intensity elicited biphasic inhibitory postsynaptic potentials (IPSPs) in both basket and bistratified cells.**

**In conclusion, basket and bistratified cells in the CA1 area show prominent differences in several of their membrane and firing properties. Both cell classes are activated by Schaffer collateral/commissural axons in a feedforward manner and receive inhibitory input from other, as yet unidentified, local-circuit neurons.** © 1996 Wiley-Liss, Inc.

**KEY WORDS: GABA, interneuron, inhibition, postsynaptic, feedforward**

## INTRODUCTION

Hippocampal interneurons, or non-principal cells, share two common properties. First, they have a dense local axonal arbor which may either target principal cells, other local-circuit neurons, or a mixture of both (Somogyi et al., 1983a; Schwartzkroin and Kunkel, 1985; Gulyás et al., 1993b; Halasy and Somogyi, 1993; Han et al., 1993; Buhl et al., 1994a,b). Second, it appears that most interneurons investigated to date store the inhibitory neurotransmitter γ-aminobutyric acid (GABA) in their terminals (Somogyi et al., 1983b, 1984, 1985; Soriano and Frotscher, 1989; Halasy and Somogyi, 1993; Halasy et al., 1996). Apart from these common characteristics, however, interneurons must be regarded as a conglomerate of heterogeneous, albeit distinct, cell classes. With respect to their anatomical properties, non-principal cells may be segregated into several categories, differing with respect to their content of peptide neurotransmitters (Somogyi et al., 1984; Kosaka et al., 1985; Sloviter and Nilaver, 1987), calcium-binding proteins (Nitsch et al., 1990; Gulyás et al., 1991), and/or efferent target profile (Somogyi et al., 1983a, 1985; Gulyás et al., 1993b; Halasy and Somogyi, 1993; Buhl et al., 1994a,b; Sík et al., 1995). However, these features are not necessarily mutually exclusive; on the contrary, for example, neurons such as the dentate gyrus hilar perforant pathway-associated (HIPP) cells (Han et al., 1993) presumably correspond to the class of somatostatin-positive hilar neurons.

With respect to their physiological properties, however, distinctions between different classes of GABAergic neuron are either blurred or are yet to be established. As yet, there is some degree of general consensus that interneurons *per se* may differ from principal cells in many of their intrinsic properties, such as short-duration ac-

Accepted for publication May 1, 1996.
Address correspondence and reprint requests to E.H. Buhl, MRC Anatomical Neuropharmacology Unit, Oxford University, Mansfield Rd., Oxford OX1 3TH, UK.

tion potentials, the absence of spike frequency adaptation, a large-amplitude fast afterhyperpolarizing potential (fAHP), or prominent outward rectification (Schwartzkroin and Mathers, 1978; Ashwood et al., 1984; Schwartzkroin and Kunkel, 1985; Misgeld and Frotscher, 1986; Lacaille and Williams, 1990; Scharfman et al., 1990; Scharfman 1992). Moreover, (some) interneurons have also been shown to differ from principal cells with respect to their glutamate receptor expression (Baude et al., 1993; McBain et al., 1994; Poncer et al., 1995) and the kinetic properties of their glutamate receptors (Livsey et al., 1993; McBain and Dingledine, 1993; Perouansky and Yaari, 1993) as well as their synaptic currents (Livsey and Vicini, 1992). There are, however, considerably fewer data available for the correlation of anatomical classes of interneurons with their physiological properties, because of the requirement for a stringent morphological or immunocytochemical identification of recorded neurons. By using such a multidisciplinary approach, it was, for example, possible to establish that fast-spiking basket cells contain the calcium-binding protein parvalbumin (Kawaguchi et al., 1987; Sík et al., 1995), whereas a bistratified cell has been shown to be calbindin immunoreactive (Sík et al., 1995). The physiological properties of interneurons have also been compared with respect to their laminar position (Kawaguchi and Hama, 1988; Lacaille and Schwartzkroin, 1988; Lacaille and Williams, 1990; Lacaille, 1991). Although these studies provided compelling evidence for the physiological heterogeneity of hippocampal non-principal cells, the relationship between the variability in physiological properties and the patterns of synaptic connections of interneurons remained elusive, largely because the hippocampal laminae are far from homogeneous with regard to their complement of GABAergic interneurons (Lacaille and Schwartzkroin, 1988; Kawaguchi and Hama, 1988; Gulyás et al., 1993b; Han et al., 1993; Buhl et al., 1994a; McBain et al., 1994).

With hippocampal layering being a relatively poor indicator of interneuronal diversity, the concept of grouping non-principal cells with respect to their efferent connectivity appears to be a more suitable approach toward categorizing GABAergic neurons (Somogyi et al., 1983a,b; Gulyás et al., 1993b; Halasy and Somogyi, 1993; Buhl et al., 1994a,b). Moreover, the advent of routinely combining *in vitro* intracellular recording techniques with correlated light and electron microscopy has now provided the opportunity to define the physiological properties and synaptic effects of interneurons which have been characterized with respect to their target selectivity (Buhl et al., 1994a,b; Buhl et al., 1995). This study will provide such a physiological comparison between two classes of GABAergic hippocampal interneurons in the pyramidal cell layer of the CA1 area. The data presented in the accompanying article (Halasy et al., 1996) demonstrate not only the GABAergic nature of basket and bistratified cells, but also distinct differences in the pattern of their afferent and efferent connections.

## MATERIALS AND METHODS

### Slice Preparation

Young adult female Wistar rats (>150 g) were deeply anesthetized with intramuscularly injected ketamine (100 mg/kg) and xylazine (10 mg/kg). Then the animals were perfused with ~30 ml of chilled artificial cerebrospinal fluid (ACSF), and their brains were removed and immersed in chilled ACSF. Using a Vibroslice (Campden Instruments, Loughborough, UK), 400-$\mu$m-thick slices were cut in the horizontal plane. The slices were transferred to a recording chamber and maintained at 34–35°C at the interface between oxygenated ACSF and a humidified atmosphere saturated with 95% $O_2$/5% $CO_2$. The flow rate was adjusted to 1.5 ml/min, and the slices were allowed to recover for >1 h. During the initial part of the experiment (perfusion, cutting, 30–45 min incubation), the ACSF was composed of (in mM) 256 sucrose, 3.0 KCl, 1.25 $NH_2P0_4$, 24 $NaHCO_4$, 2.0 $MgSO_4$, 2.0 $CaCl_2$ and 10 glucose. Subsequently, the sucrose in the ACSF was replaced by equiosmolar NaCl (126 mM). All drugs were kept as concentrated stocks, which were diluted in ACSF and then bath applied. The excitatory amino acid blockers 6-cyano-7-nitroquinoxaline-2,3-dione (CNQX) and DL-2-amino-5-phosphonopentanoic acid (AP5) were obtained from Tocris Cookson (Bristol, UK) and bicuculline hydrochloride was purchased from Sigma, (Poole, UK).

### Intracellular Recordings and Data Analysis

Micropipettes were pulled from standard wall borosilicate capillaries, filled with 2% biocytin in 1.5 M $KCH_3SO_4$, and usually beveled to a DC resistance of 80–150 MΩ. Neurons were impaled in or close to the cell body layer of the hippocampal CA1 area. Putative interneurons were identified by their distinct physiological properties (see below). Recordings were made in bridge mode using Axoclamp or modified Axoprobe (both Axon Instruments, Foster City, CA) intracellular amplifiers. Postsynaptic potentials were elicited with a fine-tipped bipolar tungsten stimulation electrode with a tip separation of ~50 $\mu$m. Data were acquired using PCM instrumentation recorders and stored on videotapes. Experimental data were redigitized at 10–20 kHz with a 12 Bit A/D board (RC Electronics Computerscope, Santa Barbara, CA) and analyzed with commercially available software (Axograph, Axon Instruments, Foster City, CA). All data are expressed as mean ± SD. Statistical analysis was performed using a non-parametric statistical test (Mann-Whitney *U*-test).

Resting membrane potentials were taken as the difference between surface DC potential following electrode withdrawal and the steady-state membrane potential without the injection of bias current. Membrane time constants were determined by fitting single exponentials to the decay of small-amplitude (<5 mV) hyperpolarizing current pulses. Similarly, input resistances were calculated from the maximum voltage deflection of small hyperpolarizing current pulses. Using rheobasic current pulses, spike amplitudes were taken from the baseline to the peak of the action potentials, while spike duration was measured at half-amplitude. The amplitudes of fAHPs were measured from the shoulder of the preceding action potentials. Whenever late AHPs were seen to follow trains of action potentials, single exponential functions were fitted to determine their decay characteristics. Variations in the rate of firing were calculated from the respective interspike intervals and numerically expressed as percent changes of the initial discharge rate. The rise time of excitatory

postsynaptic potentials (EPSPs) was determined as the interval between 10 and 90% of their respective peak amplitudes, and EPSP duration was taken at half-amplitude, excluding events that were apparently curtailed by inhibitory postsynaptic potentials (IPSPs). The time-to-peak of IPSPs was determined at depolarized membrane potentials and extrapolated from the preceding stimulus artifact.

## RESULTS

All cells included in the analysis had resting membrane potentials of minimally −55 mV without requiring hyperpolarizing bias current. Moreover, the cells remained stable for at least 30 min recording time and, upon depolarization, could fire sustained trains of high-frequency action potentials. Furthermore, only those cells were included for analysis which could be recovered for light microscopic analysis, followed by the post hoc electron microscopic scrutiny of their synaptic target profile (for full anatomical description, see accompanying article). In this regard, it has been previously established that, with respect to their efferent output, CA1 pyramidal cell layer interneurons predominantly fall into three distinct categories: axo-axonic, basket, and bistratified cells (Buhl et al., 1994a). Below, we summarize and compare the physiological properties of two types of stringently identified interneurons, basket cells (n = 13) and bistratified cells (n = 6).

### Membrane and Firing Properties

In comparison, basket cells (n = 13) had significantly more depolarized resting membrane potentials (−64.2 ± 7.2 mV) than bistratified cells (n = 6; −69.2 ±4.6 mV; $P < 0.05$). Likewise, basket cells had significantly faster membrane time constants (9.9 ± 4.6 ms) when compared to bistratified cells (18.6 ± 8.1 ms). However, although basket cells had, on average, considerably lower input impedances (31.3 ± 10.9 vs. 60.2 ± 42 MΩ in bistratified cells), this difference was not statistically significant ($P = 0.056$). Only basket cells at membrane potentials more depolarized than approximately −60 mV tended to fire spontaneous action potentials, although it should be emphasized that the sampling of neurones with extensive labeling and therefore prolonged recording periods may have biased these data toward the inclusion of cells with relatively hyperpolarized membrane potentials and, accordingly, little spontaneous activity.

Both types of interneuron had non-overshooting action potentials, the means for basket and bistratified cells being 63.6 ( ± 12.7) mV and 69.8 ±5.0) mV ($P > 0.05$), respectively. Action potentials were generally brief due to a rapid rate of fall (Fig. 1) and were found to be significantly faster in basket cells (0.41 ± 0.09 vs. 0.53 ± 0.14 ms in bistratified cells).

In response to depolarizing current pulses, both groups of neuron could display a variety of different firing patterns. Only a minority of cells fired non-accommodating trains of action potentials (Fig. 2A, D; n = 1 each; adaptation rate <10%; note: the widely used terms spike frequency accommodation and adaptation are here regarded as synonymous), although this firing pattern has commonly been associated with GABAergic interneurons (Connors and Gutnick, 1990; Scharfman, 1992). Although the majority of cells assumed a regular firing pattern, they revealed varying degrees of spike frequency adaptation, the respective changes in the rate of firing ranging from 14 to 88% (Fig. 2B; mean for all cells 42 ± 31%; n = 12) in basket cells and 20–88% (Fig. 2E; mean for all cells 54 ± 34%; n = 6) in bistratified cells. Finally, three basket (Fig. 2C) and two bistratified cells (Fig. 2F) showed a burst-like firing pattern in response to a depolarizing current pulse. Interestingly, different firing patterns may not be mutually exclusive, as they could be observed within individual cells. Accordingly, it was possible to switch cells from bursting into regular firing mode by means of a constant depolarizing current injection (Fig. 2E,F), although this property was not systematically investigated.

When the firing frequency of basket (n = 4) and bistratified (n = 3) neurons was determined from the first interspike interval, all cells revealed a linear current–frequency relationship (Fig. 3A,D). Differences, however, were apparent with respect to the slope of the individual curves; i.e., across cells, the same increment in current intensity could affect the respective firing rates to a variable degree. When current–frequency plots were determined from

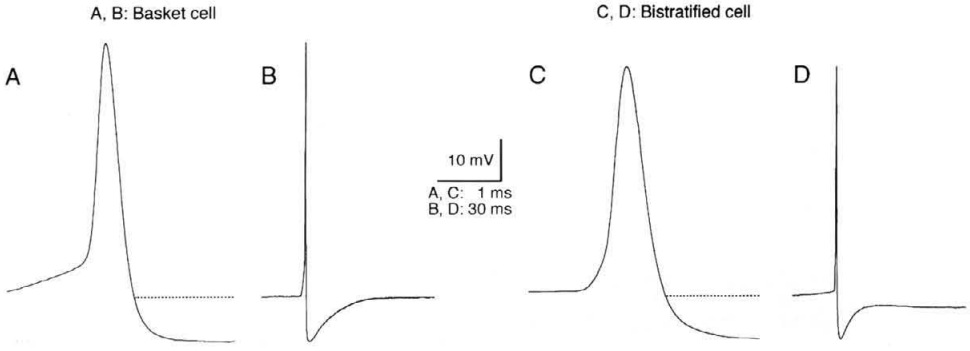


**FIGURE 1. Action potentials in both basket (A) and bistratified cells (C) are characterized by their short duration which, when measured at half-amplitude, is generally less than 600 μs. In both types of interneurons action potentials have a rapid rate of fall, which is in the same range as their rate of rise. Action potentials of basket (B) and bistratified (D) cells are followed by a short-latency fast afterhyperpolarization.**

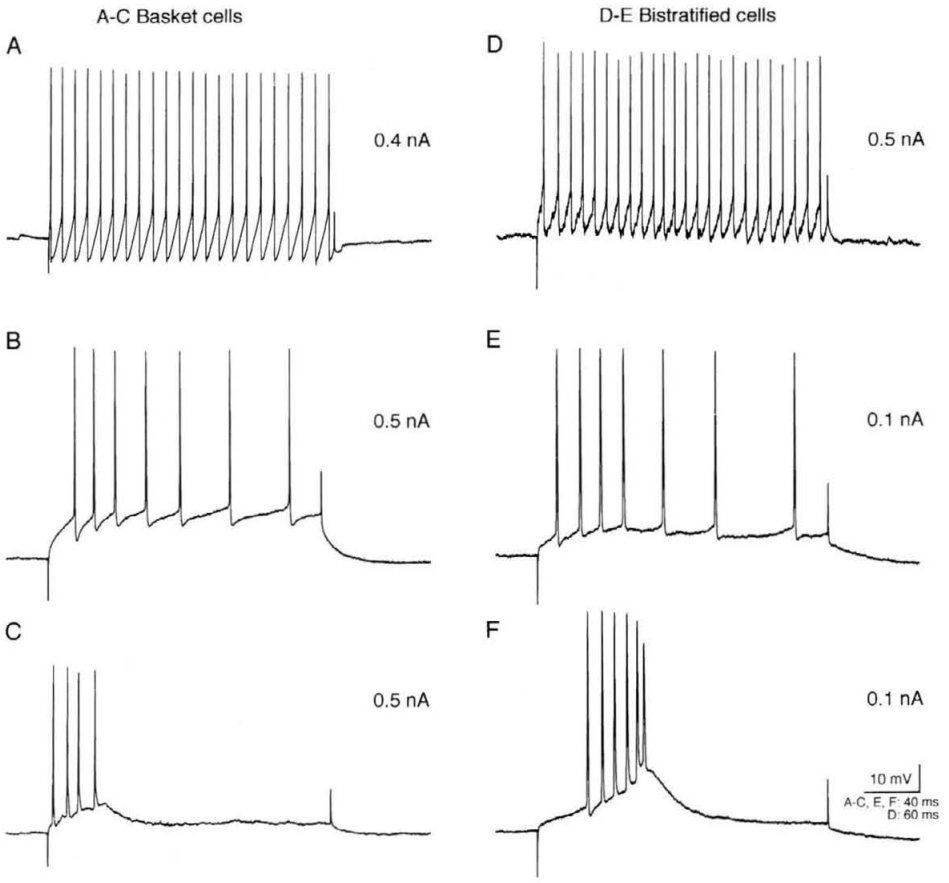


**FIGURE 2. Intrinsic firing patterns of three basket (A–C) and two bistratified cells (D–F). Within the same group of cells the firing pattern and the degree of spike frequency adaptation could vary significantly. Both basket (A) and bistratified cells (D) could discharge with a train of non-accommodating action potentials in response to a depolarizing current injection, thus corresponding to the firing pattern which is generally assumed to be associated with fast-spiking interneurons in cortical areas. Interestingly, a large proportion of both basket (B) and bistratified cells (E) showed a marked degree of spike frequency adaptation. Moreover some basket (C) and bi-stratified cells (F) were also capable of firing a burst of action potentials, which were riding on a depolarizing envelope. Note, however, that in one instance the firing mode of a bistratified cell could be changed from bursting (F) to a regular firing/adapting behavior (E) by depolarizing the cell from −62 mV (F) to −57 mV (E). The cells in A and C are also illustrated in Figures 4 and 3 of the accompanying article.**

the first and last interspike interval of 200 ms depolarizing current pulses, differences were apparent in the respective slopes of cells which exhibited marked spike frequency adaptation (Fig. 3B,E; solid symbols). Towards the end of a current pulse, these cells showed a linear, but disproportionally smaller increase in their firing rates in response to regular increases in current intensity (Fig. 3B,E; solid symbols connected by broken lines).

The regularity of neuronal discharge was assessed by plotting the respective firing frequencies, again taken as the reciprocal value of successive interspike intervals, during the injection of a constant depolarizing current pulse (Fig. 3C,F). It was clear that cells with no apparent accommodation of their firing rate maintained remarkably constant interspike intervals or discharge rates, respectively (Fig. 3C,F; open symbols). Both basket and bistratified cells which revealed marked reductions of their firing rate had relatively uniform patterns of adaptation. Thus, a sharp drop of firing rate occurred during the first 50–70 ms of the pulse, and then cells resumed discharging at a relatively constant frequency during the remainder of the pulse. Occasionally the regular firing pattern of basket (n = 1) and bistratified cells (n = 1) could be disrupted by spike doublets or triplets (Figs. 3C, 4A,D), here defined as an action potential following another with very short latency.

## Afterpotentials

Without exception, action potentials in basket and bistratified cells were followed by a short-latency fAHP (Figs. 1, 2, 4A,D). Although, on average, basket cells had more pronounced fAHPs than bistratified cells (13.5 ± 6.7 [n = 12] vs. 10.5 ± 5.1 mV [n = 6]), this difference did not reach statistical significance. Both basket and bistratified cells could reveal prominent depolarizing afterpotentials (DAPs; Fig. 4B,E; arrows). These were most prominent during the period of strongest spike frequency adaptation and could be of sufficient amplitude to trigger spike doublets and triplets (for more detail, see Buhl et al., 1994b). Only a fraction of basket cells (5/13; 39%) displayed DAPs, thus dif-

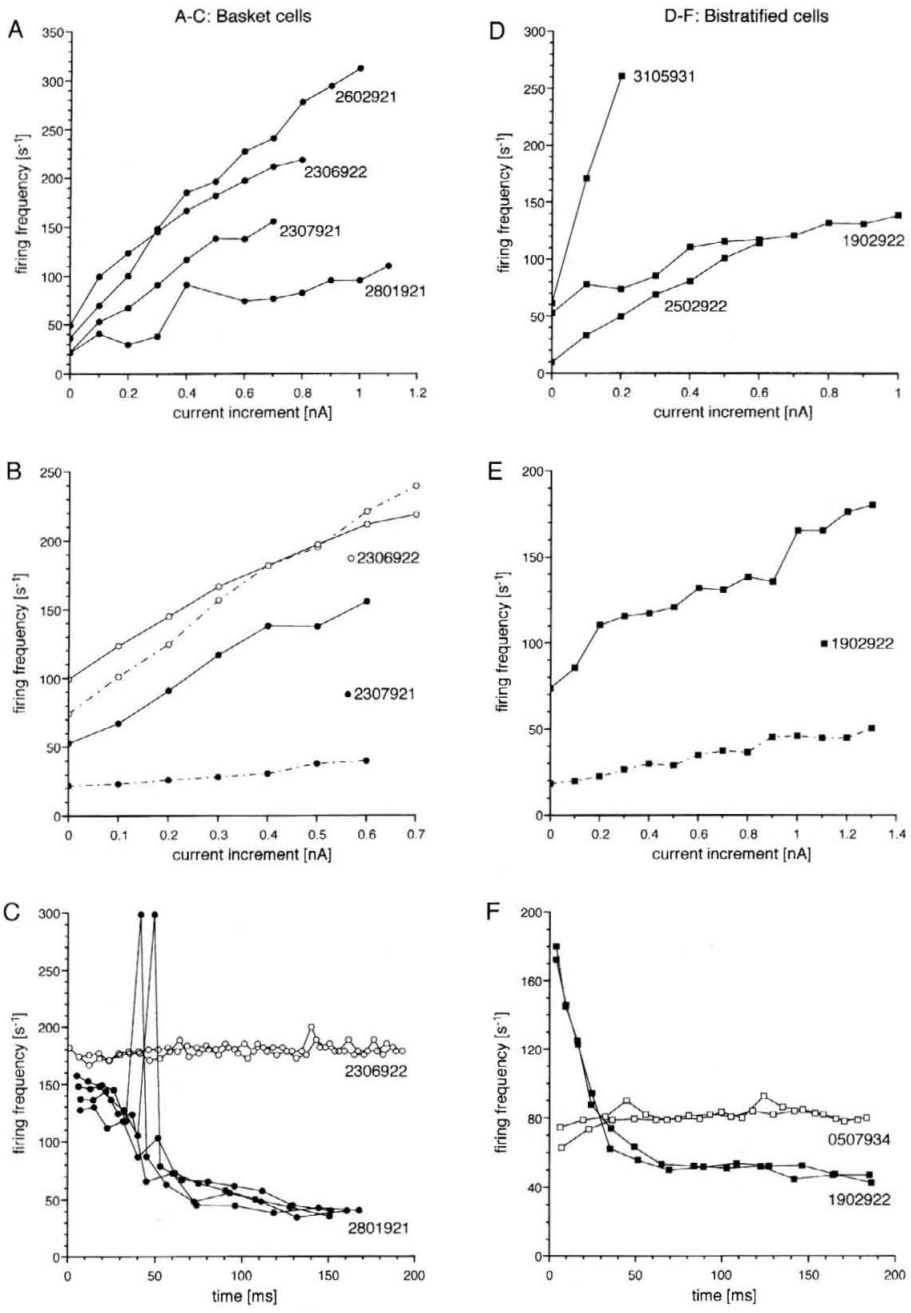


**FIGURE 3.** Firing characteristics of basket (A–C; open and solid circles) and bistratified cells (D–F; open and solid squares). The instantaneous firing frequency (expressed as the inverse of the first interspike interval [ISI]) of both basket (A) and bistratified cells (D) increased linearly with the amount of injected depolarizing current (in A,B,D,E expressed as current increment above threshold intensity). The respective slopes, i.e., the rate of frequency increase per current step, of individual cells showed great variability. In basket and bistratified cells which exhibited spike frequency adaptation (B,E: solid symbols), the respective current/frequency slopes differed markedly when taken from the first and last ISI (first ISIs connected by continuous line, last ISIs linked by broken line) of a 200-ms depolarizing current pulse. In contrast, the slopes of first and last interspike intervals in non-adapting or weakly adapting cells (B: open circles) remained relatively constant. The regularity and pattern of firing in basket (C) and bistratified cells (F) was assessed by plotting the inverse of successive interspike intervals (as a measure of firing frequency) against time. It is apparent that non-adapting cells (open symbols; two sweeps in each cell at same intensity) assume a regular firing pattern, whereas adapting cells (solid symbols; in C four sweeps at variable intensities, in F two sweeps with identical current intensity) decelerate markedly during the first 50- to 70-ms interval of the current pulse and then resume firing at near-steady-state levels. Intersweep variability was relatively minor. Only infrequently occurring doublets (C) presented a minor disruption in the overall regularity of firing patterns. When comparing two sweeps which contained doublets with two successive sweeps which were without doublets, it is, however, obvious that despite the dramatic increase in firing frequency (i.e., a very short interspike interval), the overall firing pattern remains remarkably unaffected. Cell codes correspond to Table 1 of the accompanying article.

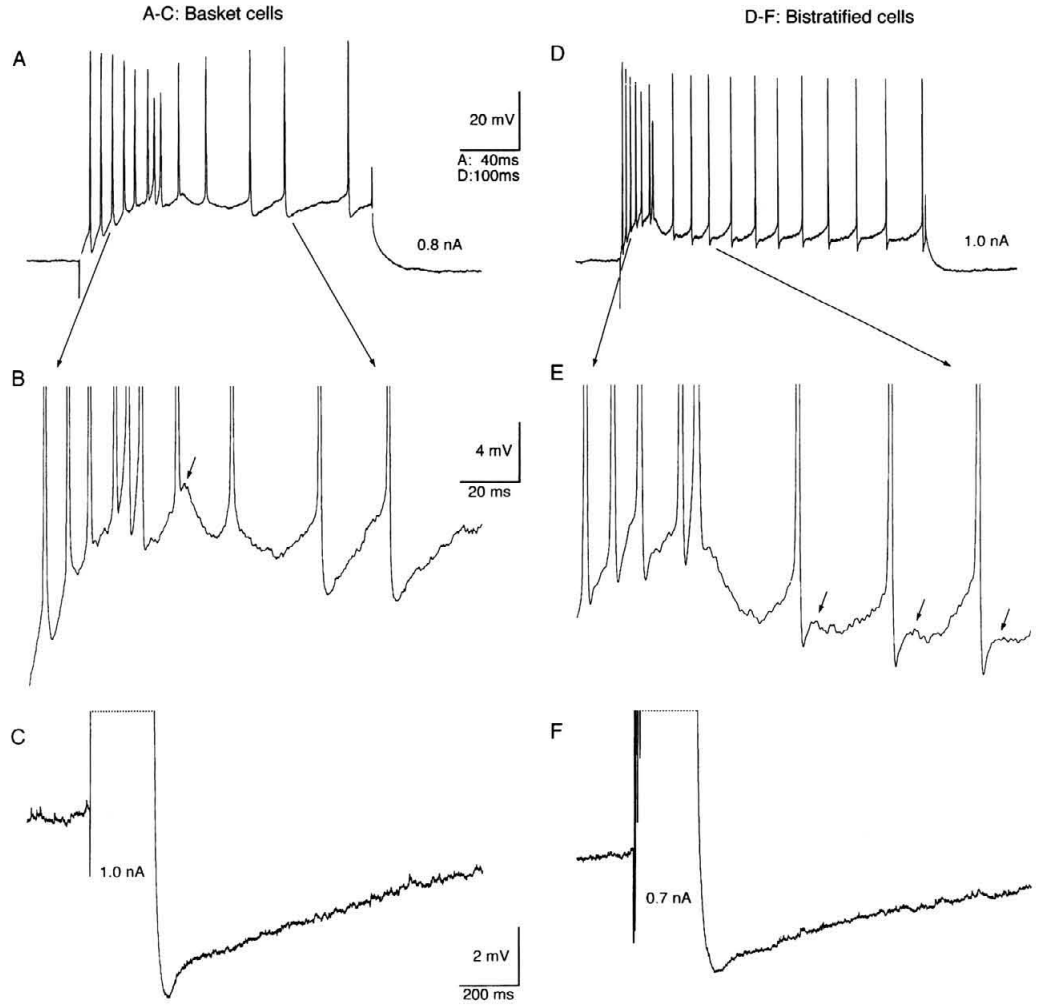


**FIGURE 4. Both basket (A–C) and bistratified cells (D–F) could show complex afterpotentials resembling those of hippocampal principal cells. In these instances a fast afterhyperpolarizing potential (see also Fig. 1B,D) was followed by a depolarizing afterpotential (DAP; B,E arrows). Occasionally DAPs were of sufficient amplitude to trigger spike doublets (D,E) or even triplets (A,B). Prominent DAPs were frequently observed in conjunction with marked frequency adaptation (A,D). Moreover, in these cells, trains of action potentials were often followed by a long-lasting afterhyperpolarization (C,F; clipping of depolarizing response indicated by stippled line; the cell in F is different from that shown in D and E). Note the clipping of action potentials in B and E. Broken lines in A indicate off-line adjustment of bridge balance. The cell in D and E is also illustrated in Figure 9 of the accompanying article.**

fering from bistratified cells where DAPs appear to be a more regular feature (5/6; 83%). Similarly, following occasionally single (Fig. 1D), but more frequently bursts of action potentials, both basket and bistratified cells could reveal prominent late afterhyperpolarizing potentials (lAHPs; Fig. 4C,F), although this feature was considerably less prominent in basket cells (n = 2/13; 15%) when compared to bistratified cells (5/6; 83%). Generally, the amplitude of lAHPs was positively correlated with the burst duration and number of action potentials. All lAHPs decayed slowly (>1 s) back to baseline, and their decay could be well fitted with a single exponential function. With respect to their respective mean time constants of decay, basket (1.24 ± 0.20 s) and bistratified cells (0.96 ± 0.97) appeared to be relatively similar. Finally, it is noteworthy that, with the exception of one bistratified cell, the occurrence of lAHPs predominantly coincided with prominent DAPs (6/7 cells).

## Postsynaptic Responses

Using low stimulation intensities, which were invariably subthreshold for concomitantly recorded pyramidal cells (data not shown), basket as well as bistratified cells could be orthodromically activated at very short latencies (<4 ms), thus minimizing the likelihood of polysynaptic pathways contributing to the early part of EPSPs. Although synaptic responses could be elicited from several stimulation sites, such as stratum lacunosum-moleculare, the data reported here resulted from placing the stimulation electrode into stratum radiatum, usually at the CA1/CA3 border region, thus presumably stimulating predominantly Schaffer collateral/commissural input fibers.

Afferent stimulation at the threshold for synaptic responses (Fig. 5A,G) invariably elicited EPSPs in basket as well as bistratified cells. The analysis of single sweeps revealed that small-amplitude

EPSPs in both types of interneurons frequently had a fragmented, multi-peaked appearance (Fig. 5G,H), the latter feature generally smoothing out in averaged traces (Fig. 5A–E). Subthreshold EPSPs in basket cells (n = 9) had an average rise-time of 1.9 ± 0.5 ms, whereas that of bistratified cells (n = 4) was determined to be 3.3 ± 1.3 ms. This difference was statistically significant ($P < 0.05$). Likewise, the mean duration of EPSPs in basket cells (10.7 ± 5.7 ms) was considerably shorter than that of bistratified cells (20.1 ± 9.7 ms), although this difference did not reach statistical significance ($P = 0.09$). When stimulating Schaffer collateral/commissural afferents with maximal intensity, all cells reached firing threshold. Suprathreshold EPSPs generally elicited one (Fig. 5E) and occasionally two action potentials.

Without exception, stimulation intensities had to be adjusted

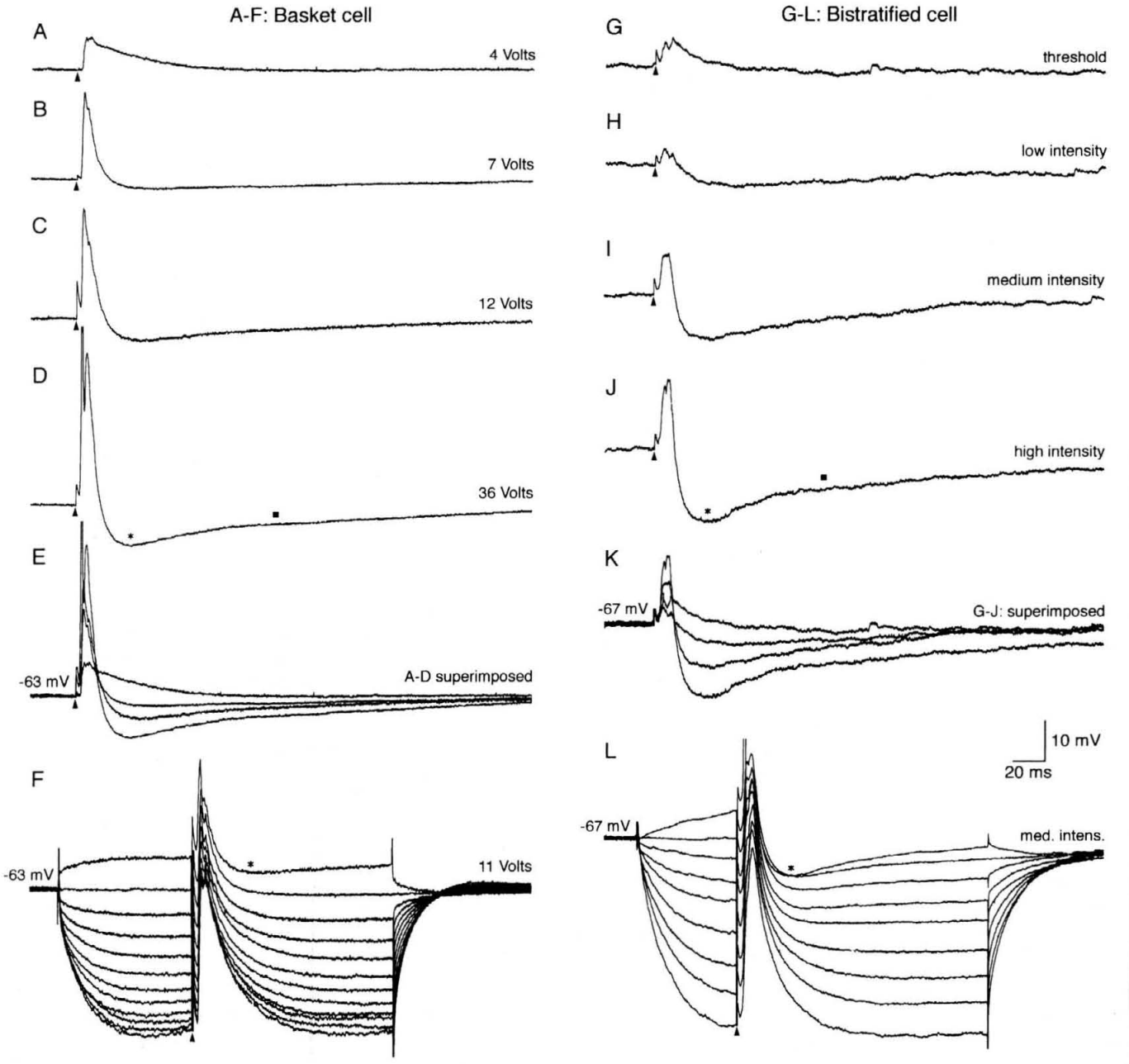


**FIGURE 5. Synaptic responses in basket (A–F) and bistratified cells (G–L) following extracellular stimulation of the Schaffer collateral/commissural pathway (arrowheads denote stimulus artifacts). Low stimulus intensities (A,G) usually resulted in excitatory postsynaptic potentials (EPSPs) without apparent inhibitory postsynaptic potentials (IPSPs). Increasing the stimulation intensity frequently recruited short-latency IPSPs (C–E, I–K; asterisks), which curtailed the duration of the EPSPs. Late IPSPs (D,J; solid squares) were only apparent at higher stimulation intensities. Traces A–F and L represent averages of four to 30 trials, G-K represent single sweeps. Note the characteristic "fragmented" appearance of EPSPs (G,H). In all tested basket (F) and bistratified cells (L) the EPSP amplitude increased with membrane hyperpolarization. Fast IPSPs (asterisks) reversed in the range of the presumed chloride equilibrium potential. The cell in A–F is also illustrated in Figure 5 of the accompanying article.**

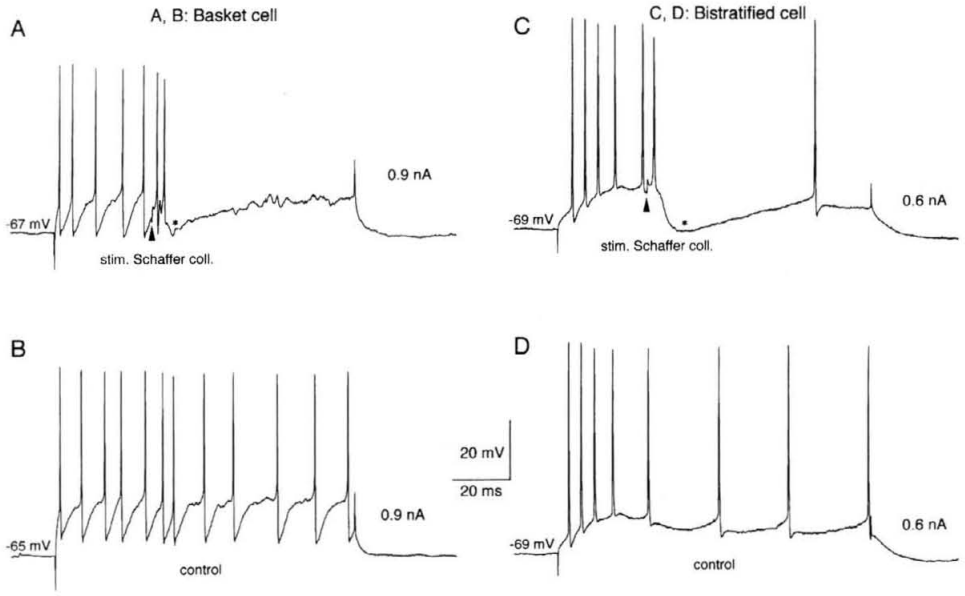


**FIGURE 6. Inhibitory responses in inhibitory cells. Schaffer collateral/commissural pathway–evoked IPSPs suppress repetitive firing in CA1 basket (A,B) and bistratified cells (C,D). Strong stimuli recruited short-latency IPSPs (asterisks) in both basket (A) and bistratified (C) cells. The resulting hyperpolarization was effective in suppressing current-induced firing for periods greater than 50 ms and frequently reducing the rate of firing during the remainder of the pulse (data not shown). The control traces (B,D) illustrate that in the absence of the synaptic stimulus, the cells fired throughout the current pulse. Note that some reduction of the firing rate of the cell shown in C and D is due to spike frequency adaptation. Arrowheads denote stimulation artifacts.**

considerably higher than response threshold to evoke fast IPSPs (Fig. 5B–D, H–J). Increasing the stimulation strength resulted in an amplitude increase of the fast IPSP and eventually, at high intensities, the appearance of a late IPSP (Fig. 5D–E, J–K). The peak latency of the fast IPSP in basket cells was 21.4 ± 4.2 ms (n = 6), which did not differ significantly from that of bistratified cells (25.7 ± 7.8 ms; n = 4). Likewise, the response reversal of the fast IPSPs in basket and bistratified cells was very similar

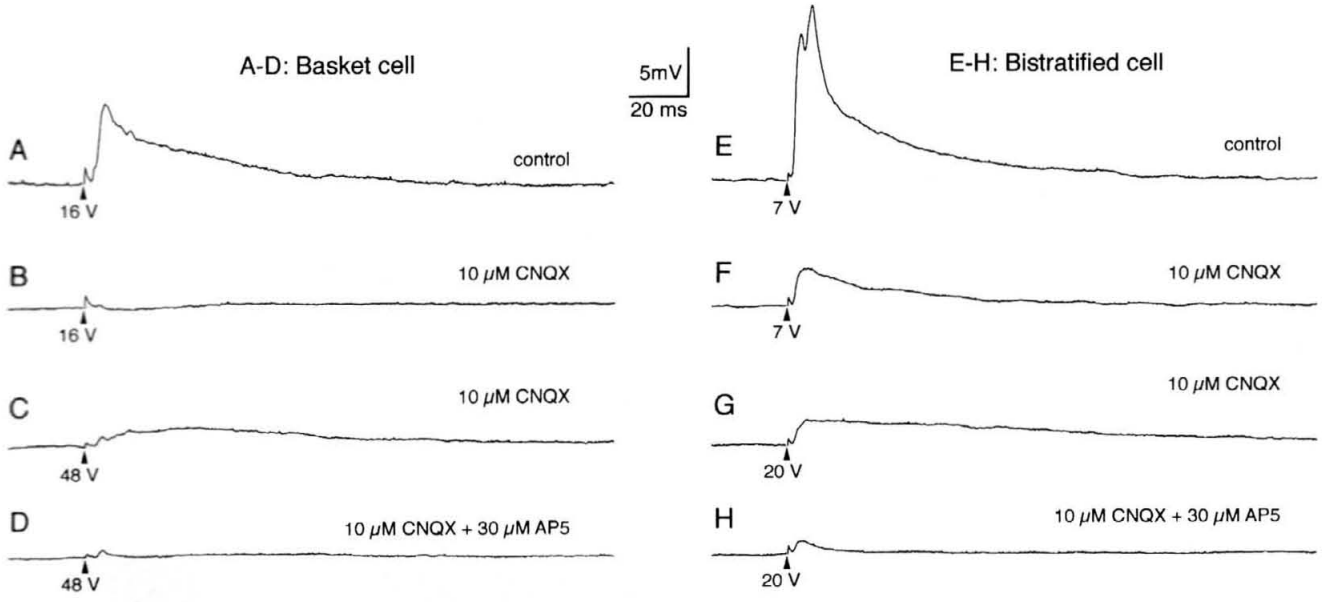


**FIGURE 7. Excitatory amino acid receptor pharmacology of Schaffer collateral/commissural pathway–evoked EPSPs in a CA1 basket (A–D) and a bistratified cell (E–H). At lower stimulation intensities, bath application of the non-NMDA receptor antagonist CNQX (10 μM) resulted in a dramatic reduction of Schaffer collateral/commissural EPSPs (A,B,E,F). In the presence of CNQX, higher stimulation intensities uncovered a CNQX-resistant EPSP with slower rise and decay kinetics (C,G). This CNQX-insensitive EPSP could be largely blocked by bath application of the NMDA receptor antagonist AP5 (D,H; 30 μM). Note that all traces in A–H were obtained in a low concentration of bicuculline (1 μM) to reduce polysynaptic IPSPs. Membrane potential in A -71 mV, in B -64 mV, in C and D -67 mV, in E and F -88 mV, and in G and H -77 mV. Arrowheads denote stimulation artifacts. The cell in A–D is also illustrated in Figure 3 of the accompanying article.**

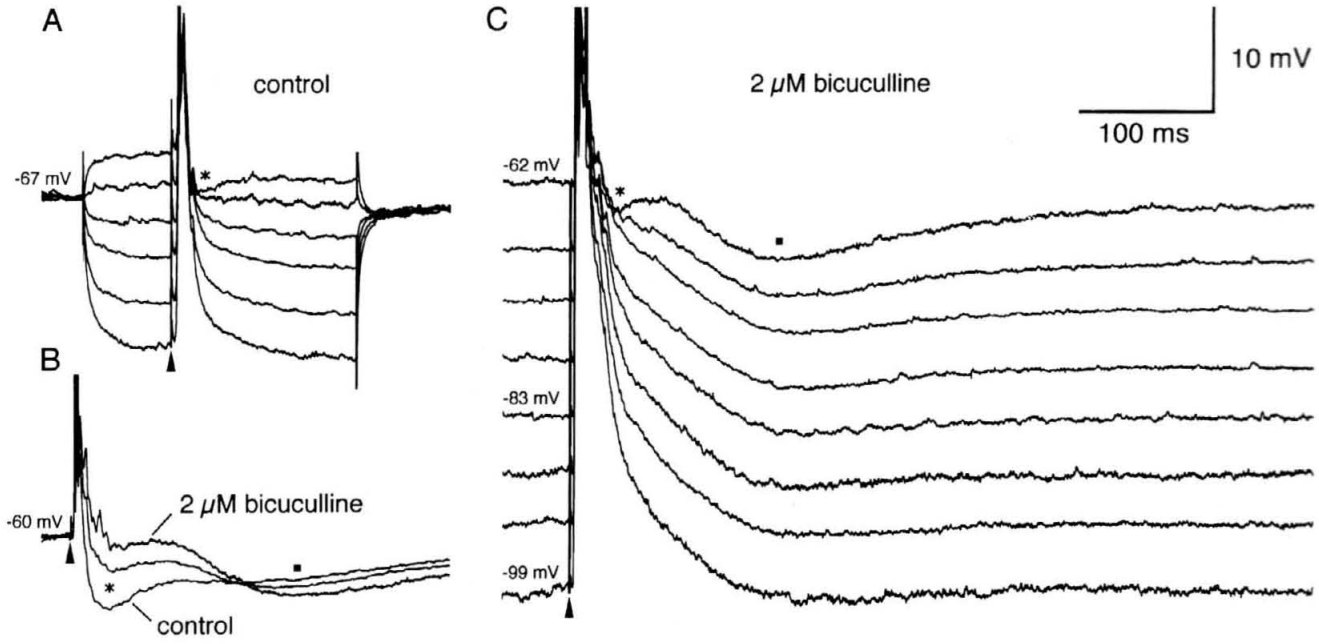


**FIGURE 8. Short-latency IPSPs in basket cells are mediated by $GABA_A$ receptors. In this basket cell the Schaffer collateral/commissural compound postsynaptic potential comprised a short-latency EPSP, which was followed by a fast IPSP (asterisks) and a late IPSP (solid square). The fast IPSP reversed around −66 mV (A), suggesting that chloride is the major charge carrier. (B) Addition of initially 1 μM (middle trace), followed by 2 μM of the $GABA_A$ receptor antagonist bicuculline methochloride to the bath, resulted in a reduction of the early IPSP and a concomitant increase of the late IPSP amplitude. Subsequently, the voltage dependency of the predominating late IPSP (C; solid square) was explored. Whereas the reversal of the small remaining early IPSP remained unchanged (C; asterisk), the late IPSP reversed around −99 mV, indicating the involvement of $GABA_B$ receptors.**

(Fig. 5F,L; −69.0 ± 2.8 vs. −72.0 ± 2.0 mV). The peak latency of the late component of the compound IPSP was 135 ± 29 ms in basket cells and 137 ± 17 ms in bistratified cells. The reversal of the late IPSP appeared to be at rather hyperpolarized membrane potentials (approx. −90 mV), although this parameter was difficult to determine unless its amplitude was enhanced following the pharmacological blockade of $GABA_A$ receptors (Fig. 8C).

The efficacy of IPSPs to inhibit firing of inhibitory neurons was tested by delivering a shock to the Schaffer/collateral commissural pathway during depolarization-induced repetitive firing in both basket and bistratified cells (Fig. 6A,C). Initially all cells responded with one to two short-latency action potentials, followed by a hyperpolarizing IPSP, which was effective in suppressing firing for periods exceeding 100 ms. Control responses at the same current intensity (Fig. 6B,D) were also analyzed to ascertain that the quiescent period was not due to a prolonged AHP following a burst-like discharge.

## Amino Acid Receptor Pharmacology

Schaffer collateral/commissural pathway–evoked EPSPs in both cell classes invariably showed a conventional voltage dependence (Fig. 5F,L), with their amplitudes increasing at more hyperpolarized membrane potentials. Such EPSPs were pharmacologically explored in three basket and three bistratified cells using subthreshold stimulation intensities (Fig. 7A and E). After monitoring the control responses for >10 min, the slices were superfused with 10 μM of the non–*N*-methyl-D-aspartate (NMDA) receptor antagonist CNQX, which could either substantially reduce or completely eliminate the evoked EPSP (Fig. 7B,F). In the presence of CNQX, a substantial increase of the stimulation intensity in conjunction with membrane depolarization could serve to uncover a residual EPSP with slower kinetics (Fig. 7C,G). This residual component proved to be sensitive to bath application of the NMDA receptor antagonist AP5 (30 μM; Fig. 7D,H).

Both the time course and reversal potential of the early phase of Schaffer collateral/commissural pathway–evoked IPSPs suggest that at least part of the compound postsynaptic response is mediated by $GABA_A$ receptors (Fig. 8A). This notion, however, could only be adequately verified in basket cells (n = 2). In the illustrated example, bath application of initially 1 μM of the $GABA_A$ receptor antagonist bicuculline resulted in a substantial reduction of the fast IPSP, whereas 2 μM diminished most of the early hyperpolarization (Fig. 8B). Interestingly, the late IPSP not only remained, but also grew in amplitude concomitant with increasing $GABA_A$ receptor blockade. Further hyperpolarization revealed that the bicuculline-resistant IPSP reversed around −99 mV (Fig. 8C).

# DISCUSSION

## Comparative Physiology of Hippocampal and Cortical Interneurons

There is general agreement that, in principle, it is possible to physiologically distinguish a substantial fraction of hippocampal interneurons from principal cells by virtue of their distinct membrane and firing properties. Differences from principal cells were

reported with respect to membrane time constants, membrane rectification, action potential duration, spike frequency adaptation, as well as afterpotentials (Ashwood et al., 1984; Schwartzkroin and Kunkel, 1985; Misgeld and Frotscher, 1986; Lacaille and Williams, 1990; Scharfman et al., 1990; Buhl et al., 1994a,b; 1995). Moreover, it was also noted that interneurons *as such* may be physiologically heterogeneous (Kawaguchi and Hama, 1988; Lacaille and Schwartzkroin, 1988). However, since the sample in these studies presumably originated from an anatomically heterogeneous pool of local-circuit neurons, it has remained unresolved whether the noted differences were due to variability *within* or *across* classes of interneurons. Indeed, recent observations on hippocampal axo-axonic cells, defined by their efferent connectivity, indicated a surprising variety of firing patterns and afterpotentials in response to depolarizing current pulses (Buhl et al., 1994b). The present study corroborated this finding by revealing a similar degree of inter-individual heterogeneity within the basket and bistratified cell classes. The majority of neurons do not correspond to the rather firmly established concept of most interneurons being non-adapting, wide-band transformators of incoming excitation, generally lacking complex afterpotentials (Connors and Gutnick, 1990; Hamill et al., 1991; Scharfman, 1992). Only a fraction of basket and bistratified cells in our sample displayed such properties. With regard to the remainder, the apparent discrepancies to previous studies may be resolved, since, in the absence of detailed morphological verification, the sampling of putative local-circuit neurons in earlier studies could have been heavily biased toward those displaying properties traditionally associated with interneurons.

Despite the aforementioned variability of physiological properties *within* given classes of hippocampal interneurons, a statistical comparison between basket and bistratified cells revealed a number of differences, among which spike duration and membrane time constant reached the level of statistical significance. In this respect, very similar parameters were recently found to segregate two populations of rat neocortical layer V interneurons, referred to as "fast-spiking" and "low-threshold spike (LTS)" cells, showing prominent differences in their membrane time constants, action potential duration, and input resistance (Kawaguchi, 1993; Deuchars and Thomson, 1995). In a similar way to cortical "fast-spiking" cells, their hippocampal equivalents have been also shown to contain the calcium-binding protein parvalbumin (Kawaguchi et al., 1987; Kawaguchi and Kubota, 1993), the latter being a marker for hippocampal basket and axo-axonic cells (Kosaka et al., 1987). Regarding their membrane and firing properties, the group of bistratified cells may correspond to cortical "LTS cells." This notion is further supported by the observation that, like the bistratified cell illustrated in Figure 2E and F, LTS cells consistently fire low-threshold spikes at hyperpolarized membrane potentials (Kawaguchi, 1993) and contain the calcium-binding protein calbindin$_{D28k}$ (Kawaguchi and Kubota, 1993), the latter being a marker for cortical interneurons with an efferent target profile enriched in dendritic shafts and spines (DeFelipe et al., 1989). Finally, further similarities between cortical LTS cells and hippocampal bistratified cells were noted by Sík et al. (1995), who demonstrated calbindin $_{D28k}$ immunoreactivity in a bistratified cell labeled *in vivo*. However, the degree of homology between these two classes of local-circuit neurons requires further assessment, owing to the recent discovery of other cortical interneurons, such as regular spiking non-pyramidal cells,with an overlapping spectrum of physiological properties (Kawaguchi, 1995).

## Schaffer Collateral/Commissural Activation of Basket and Bistratified Cells

Previous studies predicted that certain hippocampal interneurons, such as the dentate MOPP cell (Han et al., 1993), are predominantly activated in a feedforward manner, because of the complete spatial segregation of their dendrites from the recurrent axon collaterals of principal cells. In contrast, another distinct type of hippocampal interneuron, immunopositive for mGluR1$\alpha$ as well as somatostatin and projecting to the stratum lacunosum-moleculare in the CA1 area (Baude et al., 1993; McBain et al., 1994), has been shown to receive mainly recurrent pyramidal cell input (Blasco-Ibanez and Freund, 1995; Maccaferri and McBain, 1995). Although basket cells in the CA3 and CA1 regions of Ammon's horn are known to be involved in recurrent microcircuits (Gulyás et al., 1993a,b; Buhl et al., 1994a), data presented above provide clear evidence that CA1 basket cells are also activated by at least one of the major extrinsic excitatory inputs, the Schaffer collateral/commissural pathway. Likewise, bistratified and axo-axonic cells (Buhl et al., 1994b) are also involved in feedforward microcircuits. Although the latter classes of pyramidal cell layer interneurons possess a relatively large proportion of their dendrites deeply invading the oriens–alveus border region, where they mingle with the bulk of pyramidal cell axon collaterals (Buhl et al., 1994b; Halasy et al., 1996), unequivocal evidence is as yet missing as to whether these neurons also participate in recurrent microcircuits.

Both the voltage dependence and the fast kinetics of compound EPSPs resulting from the bulk stimulation of Schaffer collateral/commissural afferents indicate that these responses are largely mediated by AMPA-type glutamate receptors. And indeed, orthodromically elicited EPSPs in both basket and bistratified cells were sensitive to the action of a bath applied non-NMDA glutamate receptor antagonist. Moreover, it is reasonable to assume that much of the early AMPA receptor-mediated EPSP was of *monosynaptic* origin, owing to the considerably longer latency of disynaptically (recurrent) elicited EPSPS in CA1 interneurons (Maccaferri and McBain, 1995). However, it also appears that some of the response may have been mediated by NMDA receptors, as indicated by the slow kinetics as well as the sensitivity of the residual EPSP to a bath-applied NMDA receptor antagonist. These results thus complement previous work providing pharmacological evidence for the presence of NMDA receptors on anatomically identified CA1 axo-axonic cells (Buhl et al., 1994b). Moreover, data on hippocampal interneurons in general have repeatedly prompted very similar conclusions (Sah et al., 1990; Lacaille, 1991; McBain and Dingledine, 1993; Perouansky and Yaari, 1993).

Interestingly, basket and bistratified cells showed a significant difference in the rise time of Schaffer collateral/commissurally elicited EPSPs. Quite conceivably this EPSP parameter may have

been, at least in part, determined by the equally prominent difference in the membrane time constants of basket and bistratified cells. Several other factors may have shaped the EPSP kinetics, among them variability in the properties of AMPA receptors (Livsey and Vicini, 1992; Livsey et al., 1993) and a differential degree of electrotonic attenuation (Thurbon et al., 1994; reviewed in Spruston et al., 1994). With respect to the fast rise time of basket cell EPSPs, the *functional consequence,* following the activation of excitatory synaptic afferents, will be that basket cell action potentials will generally precede those of bistratified cells. Hence basket cell–evoked IPSPs will presumably precede those mediated by bistratified cells in postsynaptic pyramidal cells, and it is perhaps no coincidence that basket cell–mediated unitary IPSPs also have significantly faster kinetics when compared to bistratified cell effects (Buhl et al., 1994a). It therefore appears that two independent factors favor basket cells to be rather efficient in rapidly providing a perisomatic increase in membrane conductance. In contrast, the temporal properties of bistratified cell–evoked IPSPs may render them more effective in shunting NMDA receptor–mediated conductances (Staley and Mody, 1992).

## GABAergic Control of Basket and Bistratified Cells

Previous studies, using either dual recording techniques or extracellular bulk stimulation of synaptic afferents, demonstrated that physiologically and/or anatomically identified interneurons receive inhibitory input from other, as yet unidentified, local-circuit neurons (Misgeld and Frotscher, 1986; Lacaille et al., 1987; Scharfman et al., 1990; Lacaille, 1991; Buhl et al. 1994b). In this respect, basket and bistratified cells corresponded well to this general pattern, since Schaffer collateral/commissural fiber activation elicited biphasic IPSPs which were presumably mediated by both $GABA_A$ and $GABA_B$ receptors. Because basket (Deller et al., 1994) and bistratified cells are directly targeted by excitatory extrinsic afferents and have been shown to target other interneurons synaptically (Buhl et al., 1994a; Sík et al., 1995; Halasy et al., 1996), they may not only have a key role in the feedforward control of principal cells (Buzsáki, 1984; Cobb et al., 1995), but also participate in shaping neuronal activity across the GABAergic network (Buzsáki and Chrobak, 1995).

## Acknowledgments

The authors thank P. Jays, F.D. Kennedy, D. Latawiec, and J.D.B. Roberts for expert technical support, L. Lyford for secretarial assistance, and S.C. Cobb, S.V. Karnup, and V.V. Stezhka for contributing some of the experimental data. K.H. was supported by the Wellcome Trust.

## REFERENCES

Ashwood TJ, Lancaster B, Wheal HV (1984) In vivo and in vitro studies on putative interneurones in the rat hippocampus: possible mediators of feed-forward inhibition. Brain Res 293:279–291.

Baude A, Nusser Z, Roberts JDB, Mulvihill E, McIlhinney RAJ, Somogyi P (1993) The metabotropic glutamate receptor (mGluR1$\alpha$) is concentrated at perisynaptic membrane of neuronal subpopulations as detected by immunogold reaction. Neuron 11:771–787.

Blasco-Ibanez JM, Freund TF (1995) Synaptic input of horizontal interneurons in stratum oriens of the hippocampal CA1 subfield: structural basis of feed-back activation. Eur J Neurosci 7:2170–2180.

Buhl EH, Halasy K, Somogyi P (1994a) Diverse sources of hippocampal unitary inhibitory postsynaptic potentials and the number of synaptic release sites. Nature 368:823–828.

Buhl EH, Han Z-S, Lorinczi Z, Stezhka VV, Karnup SV, Somogyi P (1994b) Physiological properties of anatomically identified axo-axonic cells in the rat hippocampus. J Neurophysiol 71:1289–1307.

Buhl EH, Cobb SR, Halasy K, Somogyi P (1995) Properties of unitary IPSPs evoked by anatomically identified basket cells in the rat hippocampus. Eur J Neurosci 7:1989–2004.

Buzsáki G (1984) Feed-forward inhibition in the hippocampal formation. Prog Neurobiol 22:131–153.

Buzsáki G, Chrobak JJ (1995) Temporal structure in spatially organized neuronal ensembles: a role for interneuronal networks. Curr Opin Neurobiol 5:504–510.

Cobb SR, Buhl EH, Halasy K, Paulsen O, Somogyi P (1995) Synchronization of neuronal activity in hippocampus by individual GABAergic interneurons. Nature 378:75–78.

Connors BW, Gutnick MJ (1990) Intrinsic firing patterns of diverse neocortical neurons. Trends Neurosci 13:99–104.

DeFelipe J, Hendry SHC, Jones EG (1989) Synapses of double bouquet cells in monkey cerebral cortex visualized by calbindin immunoreactivity. Brain Res 503:49–54.

Deller T, Nitsch R, Frotscher M (1994) Associational and commissural afferents of parvalbumin-immunoreactive neurons in the rat hippocampus: a combined immunocytochemical and PHA-L study. J Comp Neurol 350:612–622.

Deuchars J, Thomson AM (1995) Single axon fast IPSPs elicited by a sparsely spiny interneuron in rat neocortex. Neuroscience 65:935–942.

Gulyás AI, Tóth K, Danos P, Freund TF (1991) Subpopulations of GABAergic neurons containing parvalbumin, calbindin D28k, and cholecystokinin in the rat hippocampus. J Comp Neurol 312:371–378.

Gulyás AI, Miles R, Sík A, Tóth K, Tamamaki N, Freund TF (1993a) Hippocampal pyramidal cells excite inhibitory neurons through a single release site. Nature 366:683–687.

Gulyás AI, Miles R, Hájos N, Freund TF (1993b) Precision and variability in postsynaptic target selection of inhibitory cells in the hippocampal CA3 region. Eur J Neurosci 5:1729–1751.

Halasy K, Somogyi P (1993) Subdivisions in the multiple GABAergic innervation of granule cells in the dentate gyrus of the rat hippocampus. Eur J Neurosci 5:411–429.

Halasy K, Buhl EH, Lörinczi Z, Tamás G, Somogyi P (1996) Synaptic target selectivity and input of GABAergic basket and bistratified interneurons in the CA1 area of the rat hippocampus. Hippocampus 6:306–329.

Hamill OP, Huguenard JR, Prince DA (1991) Patch-clamp studies of voltage-gated currents in identified neurons of the rat cerebral cortex. Cerebral Cortex 1:48–61.

Han ZS, Buhl EH, Lörinczi Z, Somogyi P (1993) A high degree of spatial selectivity in the axonal and dendritic domains of physiologically identified local-circuit neurons in the dentate gyrus of the rat hippocampus. Eur J Neurosci 5:395–410.

Kawaguchi Y (1993) Groupings of nonpyramidal and pyramidal cells with specific physiological and morphological characteristics in rat frontal cortex. J Neurophysiol 69:416–431.

Kawaguchi Y, Hama K (1988) Physiological heterogeneity of nonpyramidal cells in rat hippocampal CA1 region. Exp Brain Res 72:494–502.

Kawaguchi Y (1995) Physiological subgroups of nonpyramidal cells with specific morphological characteristics in layer II/III of rat frontal cortex. J Neurosci 15:2638–2655.

Kawaguchi Y, Kubota Y (1993) Correlation of physiological subgroupings of nonpyramidal cells with parvalbumin- and calbindin$_{D28k}$-immunoreactive neurons in layer V of rat frontal cortex. J Neurophysiol 70:387–396.

Kawaguchi Y, Katsumaru H, Kosaka T, Heizmann CW, Hama K (1987) Fast spiking cells in rat hippocampus (CA1 region) contain the calcium-binding protein parvalbumin. Brain Res 416:369–374.

Kosaka T, Kosaka K, Tateishi K, Hamaoka Y, Yanaihara N, Wu J-Y, Hama K (1985) GABAergic neurons containing CCK-8-like and/or VIP-like immunoreactivities in the rat hippocampus and dentate gyrus. J Comp Neurol 239:420–430.

Kosaka T, Katsumaru H, Hama K, Wu J-Y, Heizmann CW (1987) GABAergic neurons containing the $Ca^{2+}$-binding protein parvalbumin in the rat hippocampus and dentate gyrus. Brain Res 419:119–130.

Lacaille J-C (1991) Postsynaptic potentials mediated by excitatory and inhibitory amino acids in interneurons of stratum pyramidale of the CA1 region of rat hippocampal slices in vitro. J Neurophysiol 66: 1441–1454.

Lacaille J-C, Schwartzkroin PA (1988) Stratum lacunosum-moleculare interneurons of hippocampal CA1 region. I. Intracellular response characteristics, synaptic responses, and morphology. J Neurosci 8: 1400–1410.

Lacaille J-C, Williams S (1990) Membrane properties of interneurons in stratum oriens-alveus of the CA1 region of rat hippocampus in vitro. Neuroscience 36:349–359.

Lacaille J-C, Mueller AL, Kunkel DD, Schwartzkroin PA (1987) Local circuit interactions between oriens/alveus interneurons and CA1 pyramidal cells in hippocampal slices: electrophysiology and morphology. J Neurosci 7:1979–1993.

Livsey CT, Vicini S (1992) Slower spontaneous excitatory postsynaptic currents in spiny versus aspiny hilar neurons. Neuron 8:745–755.

Livsey CT, Costa E, Vicini S (1993) Glutamate-activated currents in outside-out patches from spiny versus aspiny hilar neurons of rat hippocampal slices. J Neurosci 13:5324–5333.

Maccaferri G, McBain CJ (1995) Passive propagation of LTD to stratum oriens-alveus inhibitory neurons modulates the temporoammonic input to the hippocampal CA1 region. Neuron 15:137–145.

McBain CJ, Dingledine R (1993) Heterogeneity of synaptic glutamate receptors on CA3 stratum-radiatum interneurones of rat hippocampus. J Physiol (Lond) 462:373–392

McBain CJ, DiChiara TJ, Kauer JA (1994) Activation of metabotropic glutamate receptors differentially affects two classes of hippocampal interneurons and potentiates excitatory synaptic transmission. J Neurosci 14:4433–4445.

Misgeld U, Frotscher M (1986) Postsynaptic-GABAergic inhibition of non-pyramidal neurons in the guinea-pig hippocampus. Neuroscience 19:193–206.

Nitsch R, Soriano E, Frotscher M (1990) The parvalbumin-containing nonpyramidal neurons in the rat hippocampus. Anat Embryol (Berl) 181:413–425.

Perouansky M, Yaari Y (1993) Kinetic properties of NMDA receptor-mediated synaptic currents in rat hippocampal pyramidal cells versus interneurones. J Physiol (Lond) 465:223–244.

Poncer J-C, Shinozaki H, Miles R (1995) Dual modulation of synaptic inhibition by distinct metabotropic glutamate receptors in the rat hippocampus. J Physiol (Lond) 485:121–134.

Sah P, Hestrin S, Nicoll RA (1990) Properties of excitatory postsynaptic currents recorded in vitro from rat hippocampal interneurones. J Physiol (Lond) 430:605–616.

Scharfman HE (1992) Differentiation of rat dentate neurons by morphology and electrophysiology in hippocampal slices: granule cells, spiny hilar cells and aspiny 'fast-spiking' cells. In: The dentate gyrus and its role in seizures (Ribak CE, Gall CM, Mody I, eds), pp 93–109. Amsterdam: Elsevier.

Scharfman HE, Kunkel DD, Schwartzkroin PA (1990) Synaptic connections of dentate granule cells and hilar neurons: results of paired intracellular recordings and intracellular horseradish peroxidase injections. Neuroscience 37:693–707.

Schwartzkroin PA, Kunkel DD (1985) Morphology of identified interneurons in the CA1 regions of guinea pig hippocampus. J Comp Neurol 232:205–218.

Schwartzkroin PA, Mathers LH (1978) Physiological and morphological identification of a nonpyramidal hippocampal cell type. Brain Res 157:1–10.

Sík A, Penttonen M, Ylinen A, Buzsáki G (1995) Hippocampal CA1 interneurons: an in vivo intracellular labeling study. J Neurosci 15: 6651–6665.

Sloviter RS, Nilaver G (1987) Immunocytochemical localization of GABA-, cholecystokinin, vasoactive intestinal polypeptide-, and somatostatin-like immunoreactivity in the area dentata and hippocampus of the rat. J Comp Neurol 256:42–60.

Somogyi P, Nunzi MG, Gorio A, Smith AD (1983a) A new type of specific interneuron in the monkey hippocampus forming synapses exclusively with the axon initial segments of pyramidal cells. Brain Res 259:137–142.

Somogyi P, Smith AD, Nunzi MG, Gorio A, Takagi H, Wu J-Y (1983b) Glutamate decarboxylase immunoreactivity in the hippocampus of the cat: distribution of immunoreactive synaptic terminals with special reference to the axon initial segment of pyramidal neurons. J Neurosci 3:1450–1468.

Somogyi P, Hodgson AJ, Smith AD, Nunzi MG, Gorio A, Wu J-Y (1984) Different populations of GABAergic neurons in the visual cortex and hippocampus of cat contain somatostatin- or cholecystokinin-immunoreactive material. J Neurosci 4:2590–2603.

Somogyi P, Freund TF, Hodgson AJ, Somogyi J, Beroukas D, Chubb IW (1985) Identified axo-axonic cells are immunoreactive for GABA in the hippocampus and visual cortex of the cat. Brain Res 332:143–149.

Soriano E, Frotscher M (1989) A GABAergic axo-axonic cell in the fascia dentata controls the main excitatory hippocampal pathway. Brain Res 503:170–174.

Spruston N, Jaffe DB, Johnston D (1994) Dendritic attenuation of synaptic potentials and currents: the role of passive membrane properties. Trends Neurosci 17:161–166.

Staley KJ, Mody I (1992) Shunting of excitatory input to dentate gyrus granule cells by a depolarizing $GABA_A$ receptor-mediated postsynaptic conductance. J Neurophysiol 68:197–212.

Thurbon D, Field A, Redman S (1994) Electrotonic profiles of interneurons in stratum pyramidale of the CA1 region of rat hippocampus. J Neurophysiol 71:1948–1958.